Iranian Journal of Science and Technology, Transactions A: Science (2019) 43:2219–2225
https://doi.org/10.1007/s40995-018-0659-9

RESEARCH PAPER

Synthesis of Silver Nanoparticles by *Clinacanthus nutans* Extract Supported with Identification of Flavonoids by UPLC-QTOF/MS and Its Antimicrobial Activity

Hazrulrizawati Abd Hamid[1] · **Roziasyahira Mutazah**[1]

Received: 10 September 2018 / Accepted: 22 November 2018 / Published online: 12 December 2018

Abstract
The present study reported a simple method in synthesizing silver nanoparticles (AgNPs) by using *Clinacanthus nutans* extract. The UV–visible spectra showed the characteristic absorption peak at 480 nm, and the intensity was increased with the increase in plant extract ratio and incubation period. Analysis of particle size through FESEM, XRD and TEM revealed the average of synthesized AgNPs is 73.4 nm. The EDX analysis confirmed the formation of metallic nature of silver. The FTIR spectra indicated the role of carbonyl groups in the synthetic process and further confirmed by identification of flavonoids and their glycosides by UPLC-QTOF/MS. Antimicrobial activity of biosynthesized AgNPs shows effective inhibition against common bacterial strains including *Bacillus subtilis*, *Enterococcus faecalis*, *Staphylococcus aureus*, *Escherichia coli*, *Pseudomonas aeruginosa* and *Proteus vulgaris.*

Keywords Silver nanoparticles · *Clinacanthus nutans* · Antimicrobial activity · UPLC-QTOF/MS · Flavonoids

1 Introduction

The advancement of nanotechnologies has been an emerging research area due to their wide applicability to almost every field of science and technology. In the nanotechnology industry, a number of promising products including silver, gold, alumina and copper oxide are widely synthesized, for variety applications. Silver has gained the highest interest since it discovered to exhibit an outstanding bactericidal and fungicidal activity in comparison with other metals (Rana and Kalaichelvan 2011). Silver metals are established to have potent antimicrobial efficacy against a wide range of over 650 microorganisms from different classes including bacteria, fungi, viruses and eukaryotic microorganisms. The antimicrobial efficacy improves when the silver particles are developed in nanoscale regime, as it shows a larger surface area to volume ratio (Gong et al. 2007). Conventional chemical and physical methods to synthesis silver nanoparticles have disadvantages such as the use of hazardous reagents, toxicity, high cost and high energy consumption. Synthesis of nanoparticles by using plant extracts is preferred as it is cost effective. Ecological benign approach and the materials are easily available. *Clinacanthus nutans* Lindau that belongs to the family of Acanthaceae is a small shrub native to tropical Asian countries. The extracts of leaves of *C. nutans* have been extensively used as primary sources of complementary healthcare as economical in-house regimens for cancer patients (P'ng et al. 2012). The biomolecules and secondary metabolites of plants contributed to the reduction and stabilization of silver ions throughout the biosynthetic process (Ahmed et al. 2016).

Thus, in the present paper, we analyze the ability of methanol extract of *C. nutans* to synthesize Ag nanoparticles supported with chemical profiling by UPLC-QTOF/MS and their antimicrobial activity.

2 Materials and Method

2.1 Preparation of Plant Extract

The leaves were collected in Jelebu, Negeri Sembilan. The plant was authenticated by Dr. Shamsul Kamis, from

✉ Hazrulrizawati Abd Hamid
hazrulrizawati@ump.edu.my

[1] Faculty of Industrial Sciences and Technology, Universiti Malaysia Pahang, Lebuhraya Tun Razak, 26300 Gambang Kuantan, Pahang, Malaysia

Institute of Bioscience, Universiti Putra Malaysia. A voucher specimen number (SK 2874/75) was deposited at the Herbarium Unit of Universiti Putra Malaysia, Malaysia. Dried leaves were sonicated for 30 min at below 60 °C. This process was repeated three times. Methanol extract was filtered and evaporated to dryness and stored at 4 °C for further study.

2.2 Chemical Profiling by UPLC-QTOF/MS

Chemical profiling of active ingredients in *C. nutans* methanolic extract was done by using Waters ACQUITY UPLC-QTOF/MS I-Class systems (Waters, Milford, USA) equipped with a binary pump, an autosampler, a degasser and a diode-array detector (DAD). The system was controlled with Waters UNIFI Vion software. The chromatographic column UPLC-QTOF/MS HSS T3 C18 (2.1 mm × 100 mm, 1.8 µm) was used and eluted with a linear gradient of A (0.1% formic acid in deionized water) and B (ACN) at a flow rate of 0.5 mL/min for 16 min (Hamid et al. 2017). The injection volume was 3 µL.

2.3 Synthesis of Silver Nanoparticles

Clinacanthus nutans methanolic plant extract was prepared and added to 1.0 mM of $AgNO_3$ solution in different volume ratios as follows: 1: 50, 2: 50, 3: 50, 4: 50 and 5: 50 mL. Five samples were prepared and incubated for 48 h in an ambient shaker incubator (Protech, Model SI-100D) with 200 rpm at 37 °C. At the time intervals of 24 h, 15 mL of each mixture was centrifuged in refrigerated centrifuge (Kubota, Model 5922) at 6000 rpm for 15 min to eliminate the unwanted biomolecules. Subsequently, the pellet was re-dispersed with deionized water after discarding the supernatant and dried in oven at 50 °C for 24 h. The centrifugation and drying procedures were repeated after the mixtures experienced 48 h incubation.

2.4 Characterization of Silver Nanoparticles

The biosynthesis of the AgNPs in various mixtures was monitored by measuring the UV–visible spectra from 380 to 700 nm at room temperature. The dried AgNPs were diluted with chloroform and subjected to attenuated total reflectance Fourier transform infrared spectroscopy (ATR-FTIR). The field emission scanning electron microscope (FESEM) and attached energy-dispersive X-ray detector were used to analyze the structure and composition of biosynthesized nanoparticles. The powder X-ray diffraction data of silver nanoparticles were measured by XRD. The particle size and morphology of synthesized AgNPs were analyzed using transmission electron microscopy (TEM).

2.5 Antimicrobial Activity

Antimicrobial activity of AgNPs was conducted against three Gram-positive strains: *B. subtilis* (ATCC 11774), *Enterococcus faecalis* (ATCC 14506) and *Staphylococcus aureus* (ATCC BAA 1026), and three Gram-negative strains: *Escherichia coli* (ATCC 10536), *Psuedomonas aeurogenosa* (ATCC 1542) and *Proteus vulgaris* (ATCC 33420) using disk diffusion method (Standards and Jorgensen 1993; Wayne 2002). Mueller-Hinton broth was used to subculture bacteria and was incubated at 37 °C for 24 h. The bacterial suspension was adjusted to match density as 0.5 McFarland standard. Fresh overnight cultures with a suspension of the tested microorganism (0.1 ml of 10^8cells/ml) were taken and spread on the agar plates to cultivate bacteria. Sterile filter paper disks of 6 mm diameter were impregnated with 10 µL aqueous AgNPs (1000 ppm). Plates containing media as well as cultures were divided into four equal parts, and previously prepared disks were placed on each part of the plate. The disk soaked with distilled water was utilized as the negative control, and disk soaked with amphotericin-B (300 ppm) was used as the positive control. All of the plates were incubated at 37 °C for 24 h, and the diameters of the inhibition zones around the disk impregnated with AgNPs were measured in mm.

3 Results and Discussion

In this study, it is important to develop a robust method for the chemical profiling of the *C. nutans* methanolic extract. UPLC-QTOF/MS analysis was carried out to identify the active ingredients in the plant extract, which participated in biosynthesis of silver nanoparticles. The peak identification was performed by comparing the retention time (RT), mass error, ion response and fragmentation pattern for each compound. Since all fragment ions were automatically elucidated by MassFragment, the verification process for the components became easier. Based on the data processing in UNIFI software, the components are classified as a good match with ± 5 mDa error and poor match with ± 10 mDa error. In order to verify if a match is reasonable, the adduct ions as well as the fragmentation ions were studied. The element compositions were inferred in the light of high-accuracy molecular ions within the mass error of 5 mDa and ion response more than 80,000 (Hamid et al. 2018). Then, by reviewing the MS/MS fragmentation ions and relevant reference literatures, their chemical structures were further verified. Although 53 compounds were listed as good match, only six compounds were labeled as confirmed (Table 1).

Table 1 Tentative identification of flavonoids from *C. nutans* extract

Component name	Observed (m/z)	Mass error (mDa)	Observe RT (min)	Response
5,7-Dihydroxychromone-7-β-D-glucoside	340.0718	3.2	4.36	166,170
Smiglanin	340.0720	3.3	4.94	84,088
Glabrol	393.2098	3.8	6.63	100,003
Corymboside	565.1564	1.2	7.6	216,303
Viscumneoside II	535.1452	0.6	8.69	129,730
Kushenol U	422.2033	4.8	11.27	141,927

Peaks with retention times (RT; min) of 4.36, 4.94, 6.63, 7.60, 8.69 and 11.27 were identified as follows: 5,7-dihydroxychromone-7-β-D-glucoside, smiglanin, glabrol, corymboside, viscumneoside II and kushenol U (Fig. 1). Although the compounds identified are not similar as the compounds reported by (Teshima et al. 1997), the basic rings that were identified are similar. Most of the compounds are flavones and their glycosides. The fragmentation pathway of corymboside leads to the loss of small molecules CO with m/z 511.12431 and produces low m/z 272.04442 for aglycones. The partial cleavage at the glycosidic linkages was determined at m/z 427.10277 and fragmentation at m/z 379.08168, suggesting that the compound had an additional substituent group of glycoside. Compounds glabrol and kushenol U possess prenyl group attached to the flavone ring. Compound glabrol $[M+H]^+$ ion at m/z 393.2098 and kushenol U $[M+H]^+$ ion at m/z 422.2033 have maximum intensity (100%), which indicates high ion stability. Compounds viscumneoside II $[M+H]^+$ ion at m/z 535.1452 and 5,7-dihydroxychromone-7-β-D-glucoside $[M+H]^+$ ion at m/z 340.0718 and smiglanin $[M+H]^+$ 343.072 showed the cleavage at the glycosidic linkage and produced low m/z in their aglycones suggesting that they contain one glycoside group.

Based on this information, the identified components could be categorized into flavonoids group. Flavonoid compounds play a principal role in bio-reduction of silver ions. Based on the FTIR spectroscopy data, various functional groups namely carbonyl group and hydroxyl group could be found in flavonoids (Hazrulrizawati and Zeyohannes 2017). It had been suggested that mechanism of bio-reduction by polyphenolic compounds was initiated with tautomerization. The release of a reactive hydrogen atom during tautomeric transformation from enol-form to the keto-form was possibly involved in the reduction of silver ions into silver nanoparticles (Makarov et al. 2014). In addition, redox mechanism might be the key role of the ketone groups in the identified compounds that reduced the silver ions into elemental silver, by conversion into carboxylic groups. According to Symonowicz and Kolanek (2012), interactions of some flavonoids with metal ions could lead to chelate formation by using their carbonyl groups or π electrons and hydroxyl groups as coordination sites. For example, corymboside could chelate between 4-carbonyl and 5-hydroxyl groups and between two

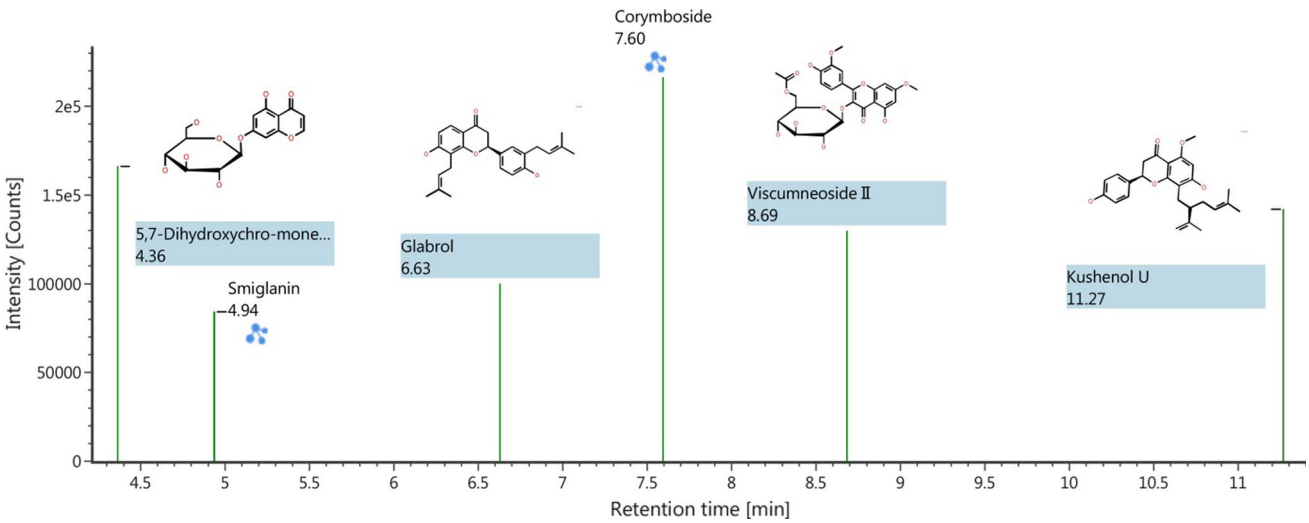

Fig. 1 Confirmed component plot of methanol *C. nutans* extract

hydroxyl groups at other sites. Such mechanisms probably explained on the ability of flavonoids compounds on acting as capping agents and subsequently induced the formation of silver nanoparticles.

The color intensity of the reaction mixture was gradually turning into light reddish brown after 1 h, 24 h and 48 h of incubation period, respectively (Fig. 2a). Absorbance intensity increased with increasing extract and incubation time because the availability of biomolecules and reaction time required for the reduction of silver ions to silver nanoparticles are more and result in the formation of more AgNPs. The increase in absorbance with color intensity could be ascribed to the increase in the amount of silver nanoparticles as the time prolonged. This rapid generation of AgNPs in reaction mixture was owing to the great reducing potential of the active components in *C. nutans* extract.

The electronic transitions involving the Ag^{+} ion give rise to absorption bands located between 200 and 230 nm, whereas the electronic transitions of metallic Ag^{0} appear in the 250–330 nm spectral range (Lu et al. 2005). In this analysis, a characteristic absorption peak was observed at 480 nm. According to Sun and Xia (2003), the presence of absorption peak at 480 nm was attributed to the silver nanoparticles of the size of around 80 nm, and this statement was further verified by FESEM analysis.

The increase in absorbance with color intensity could be due to the increase in the amount of silver nanoparticles as the time prolonged (Fig. 2b). This rapid generation of AgNPs in reaction mixture was owing to the great reducing potential of the active components in *C. nutans* methanolic extract. The absorption peaks increase as the volume of the *C. nutans* methanol extract increased from 1 to 5 mL (Fig. 2c). The broader wavelength and tailing at the longer wavelength indicated the enhancement of the particle size (Vigneshwaran et al. 2007).

The topographical image of synthesized AgNPs at different magnification is shown in Fig. 3. High density of silver nanoparticles synthesized by *C. nutans* could be observed and aggregated due to the capping of phytoconstituent over the AgNPs. The development of the silver nanostructures was further confirmed as spherical shape and clearly distinguishable in 77.8–85.3 nm in size. The EDX analysis

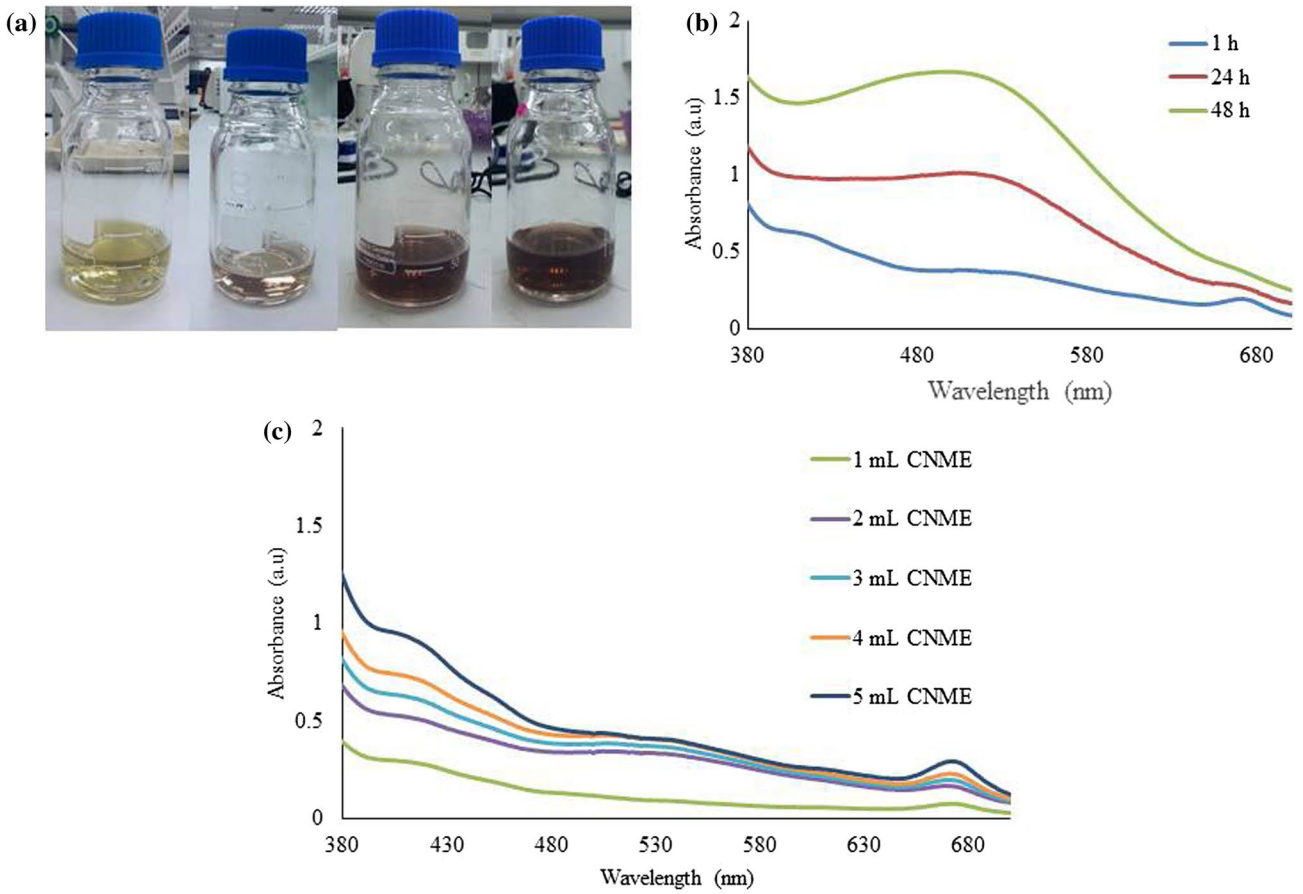

Fig. 2 **a** Reaction mixtures before (i) and after incubation (ii)1 h, (iii) 24 h (iv) 48 h, **b** UV–Vis absorption spectra at different time intervals and **c** UV–visible absorption spectra at different volume of CNME

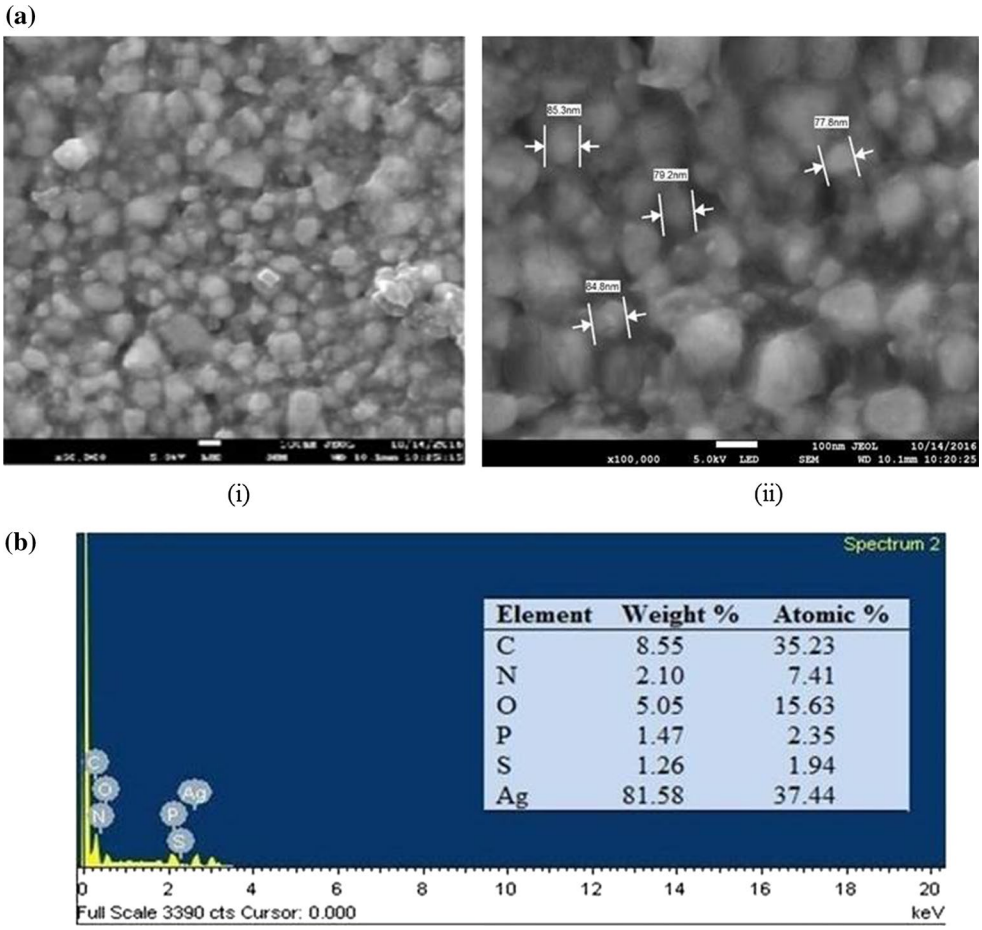

Fig. 3 **a** FESEM micrograph at different magnification (i) 20 kx and (ii) 100 kx and **b** EDX spectrum and elemental analysis of AgNPs

(Fig. 3b) showed a significant peak of silver, which was indicated at around 2.7 keV. Formation of AgNPs was confirmed as typical optical absorption peak of metallic silver nanoparticles that generally takes place approximately at 3 keV (Bindhu and Umadevi 2013). Silver was appeared as the major constituent, which was 81.58% of total weight of the sample. The presence of peaks of C, N, O, P and S corresponded to organic moieties that exist in *C. nutans* extract. These elements were the active molecules of *C. nutans* responsible for bio-reduction of silver ions to elemental silver.

X-ray diffraction (XRD) pattern of AgNPs is shown in Fig. 4. Four diffraction peaks at 2θ values of 38°, 44°, 64° and 77° are indexed to the planes of (111), (200), (220) and (311) reflections of the fcc (face centered cubic) structure of crystalline silver. The diffraction pattern indicates the biosynthesis of AgNPs. XRD size calculation based on Scherrer equation shows the particle size of AgNPs were in the range 84.8–92.3 nm. Particle size calculated by Scherrer not always gives a real crystallinity size value because the full width at half maximum (FWHM) was affected not only by the particle size but also by the structural strain. The size, shape and morphology of biosynthesized silver

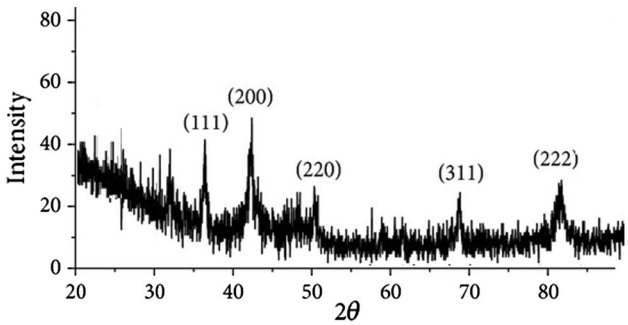

Fig. 4 XRD pattern of AgNPs obtained by *C. nutans* extract

nanoparticles were further interpreted with the help of transmission electron microscopy (TEM).

Figure 5 shows TEM micrographs of AgNPs synthesized by using *C. nutans* extract. The TEM images confirmed the formation of AgNPs with particle size of 46.4–53.8 nm. The edge of particles was lighter than the centers suggesting that biomolecules in *C. nutans* extract capped the AgNPs. Based on comparison between

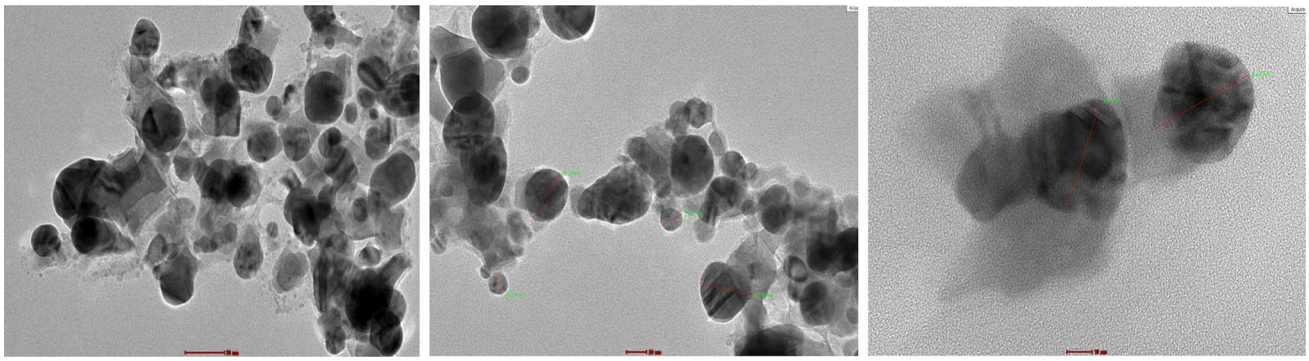

Fig. 5 TEM micrographs of AgNPs synthesized by using *C. nutans* extract

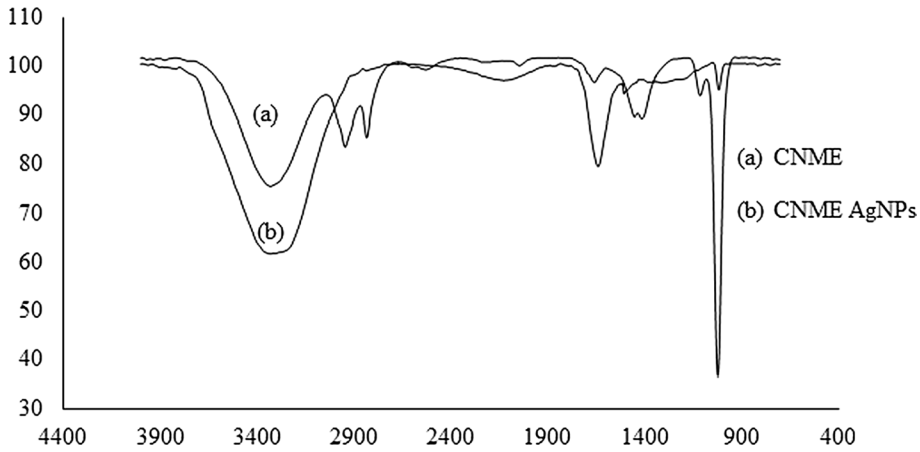

Fig. 6 FTIR spectra of CNME and CNME-AgNPs

FESEM, XRD and TEM, it can be concluded the particle size of synthesized AgNPs is in average 73.4 nm.

The FTIR spectra of *C. nutans* methanol extract and CNME-AgNPs sample are shown in Fig. 6. In the CNME, absorption peaks were observed at 3328.76 cm^{-1} indicating the O–H stretching of alcohols, sharp peak at 1021.11 cm^{-1} designates the C–O stretching, small peak at 2944.09 cm^{-1} indicates the C–H stretching, 1412.86 cm^{-1} for C=C stretching, and small peak at 1657.08 cm^{-1} denotes the C=O functional group.

In comparison with the spectra of the CNME-AgNPs sample, C–O stretch had showed a decrease in intensity, indicating the involvement of C–O group in biosynthesis of AgNPs and shift to lower wave number due to binding of the functional groups with the silver nanoparticles surface. Carbonyl group was considered as one of the active components in involving bio-reduction of silver ions, and it could be attributed to the flavonoids group in *C. nutans*. This finding was in agreement with reported phytochemicals in *C. nutans* that indicate the presence of steroids, C-glycosyl flavones, sulfur-containing glycosides, glycoglycerolipids, cerebroside and monoacyl monogalactosyl glycerol (Alam et al. 2016). The absorbance intensity of O–H and C–O showed increment due to hydrolysis of polysaccharides in the plant and deionization of water used in the silver nitrate solution.

Table 2 Results of antimicrobial activity of CNME-AgNPs

Bacterial strain	Zone of inhibition (mm)		AgNPs
	Positive control (Gentamicin)	Negative control (CNME)	
B. subtilis	30.00 ± 0.03	6.00 ± 0.27	11.50 ± 1.22
E. faecalis	20.00 ± 0.01	6.00 ± 0.45	8.33 ± 0.47
S. aureus	19.00 ± 0.03	5.80 ± 0.25	8.67 ± 0.82
E. coli	19.00 ± 0.04	6.00 ± 0.30	8.50 ± 0.50
P. aeruginosa	21.00 ± 0.02	6.00 ± 0.34	9.00 ± 0.94
P. vulgaris	20.00 ± 0.03	5.80 ± 0.45	8.80 ± 0.45

In this study, AgNPs showed the remarkable inhibitory effect on all tested bacteria (Table 2). In comparison, AgNPs revealed a better antimicrobial efficacy on gram-positive bacteria as larger diameter of zone of inhibition possessed on *B. subtilis* as compared to the gram-negative bacteria.

Gram-positive bacteria exhibited larger susceptibility due to the presence of peptidoglycan layers, which allow the penetration of foreign substances without any barrier

(Shah et al. 2018). The membrane structure of gram-negative bacteria contains lipopolysaccharides served as a protective barrier for the cell from complement-mediated lysis from various antibiotics. The mechanism of the antimicrobial activities of silver nanoparticles is still investigated and well debated. One of the widely recognized antimicrobial mechanisms was the inhibitory effect of silver ions against the microorganisms due to electrostatic attraction. Penetration followed by disruption of cell wall or cell membrane occurs when positively charged nanoparticles are attached to the negatively charged microorganism (Cao et al. 2001).

4 Conclusion

In summary, the present work exposes a simple biosynthetic method of AgNPs by using methanol extract of C. nutans at room temperature. The synthetic strategy for this study demonstrated one-step simple process that was using eco-friendly reducing agents. The products are free from chemical contamination and not related to toxicity issue as compared to the findings by c-Esparza et al. (2016) which used the chemical reagents. Although the particle size is unable to be controlled as what had been proposed by Panáček et al. (2006), the synthesized AgNPs were stable and spherical in shape with average particle size 73.4 nm. The particle size of synthesized AgNPs had been confirmed by FESEM-EDX, XRD and TEM. Moreover, this approach was easily scaled up and was relatively low cost than physical and chemical syntheses. To the best of our knowledge, this is the first time the information of AgNPs was accomplished by using *C. nutans* as reducing agent with the profiling of phenolic compounds by UPLC/QTOF-MS. The present investigations might broader the application of *C. nutans* not only for cancer prevention plants but also to be potentially used to synthesis silver nanoparticles. The synthesized nanoparticles have the potential for antimicrobial activity and therefore can be used in pharmaceutical applications.

Acknowledgements Our sincere appreciation to the Universiti Malaysia Pahang for their support and granting research grant RDU170356 to HA Hamid.

References

Ahmed S, Ahmad M, Swami BL, Ikram S (2016) A review on plants extract mediated synthesis of silver nanoparticles for antimicrobial applications: a green expertise. J Adv Res 7:17–28

Alam A, Ferdosh S, Ghafoor K, Hakim A, Juraimi AS, Khatib A, Sarker ZI (2016) *Clinacanthus nutans*: a review of the medicinal uses, pharmacology and phytochemistry. Asian Pac J Trop Med 9:402–409

Bindhu M, Umadevi M (2013) Synthesis of monodispersed silver nanoparticles using Hibiscus cannabinus leaf extract and its antimicrobial activity. Spectrochim Acta Part A Mol Biomol Spectrosc 101:184–190

Cao Y, Jin R, Mirkin CA (2001) DNA-modified core – shell Ag/Au nanoparticles. J Am Chem Soc 123:7961–7962

Gong P et al (2007) Preparation and antibacterial activity of Fe_3O_4@Ag nanoparticles. Nanotechnology 18:285604

Hamid HA, Mutazah R, Yusoff MM, Karim NAA, Razis AFA (2017) Comparative analysis of antioxidant and antiproliferative activities of *Rhodomyrtus tomentosa* extracts prepared with various solvents. Food Chem Toxicol 108:451–457

Hamid HA, Ramli ANM, Zamri N, Yusoff MM (2018) UPLC-QTOF/MS-based phenolic profiling of Melastomataceae, their antioxidant activity and cytotoxic effects against human breast cancer cell MDA-MB-231. Food Chem 265:253–259

Hazrulrizawati H, Zeyohannes SS (2017) *Rhodomyrtus Tomentosa*: a phytochemical and pharmacological review. Asian J Pharm Clin Res 10:1–7

López-Esparza J, Espinosa-Cristóbal LNF, Donohue-Cornejo A, Reyes-López SNY (2016) Antimicrobial activity of silver nanoparticles in polycaprolactone nanofibers against gram-positive and gram-negative bacteria. Ind Eng Chem Res 55:12532–12538

Lu J, Bravo-Suárez JJ, Takahashi A, Haruta M, Oyama ST (2005) In situ UV–Vis studies of the effect of particle size on the epoxidation of ethylene and propylene on supported silver catalysts with molecular oxygen. J Catal 232:85–95

Makarov V, Love A, Sinitsyna O, Makarova S, Yaminsky I, Taliansky M, Kalinina N (2014) "Green" nanotechnologies: synthesis of metal nanoparticles using plants. Acta Naturae (англоязычная версия) 6

Panáček A et al (2006) Silver colloid nanoparticles: synthesis, characterization, and their antibacterial activity. J Phys Chem B 110:16248–16253

P'ng XW, Akowuah GA, Chin JH (2012) Acute oral toxicity study of *Clinacanthus nutans* in mice. Int J Pharm Sci Res 3:4202

Rana S, Kalaichelvan P (2011) Antibacterial activities of metal nanoparticles. Antibact Act Metal Nanoparticles 11:21–23

Shah S, Ukaegbu C, Hamid H, Alara O (2018) Evaluation of antioxidant and antibacterial activities of the stems of *Flammulina velutipes* and *Hypsizygus tessellatus* (white and brown var.) extracted with different solvents. J Food Meas Charact 12:1947–1961

Standards NCFCL, Jorgensen JH (1993) Performance standards for antimicrobial disk susceptibility tests. National Committee for Clinical Laboratory Standards

Sun Y, Xia Y (2003) Gold and silver nanoparticles: a class of chromophores with colors tunable in the range from 400 to 750 nm. Analyst 128:686–691

Symonowicz M, Kolanek M (2012) Flavonoids and their properties to form chelate complexes. Biotechnol Food Sci 76:35–41

Teshima K-i, Kaneko T, Ohtani K, Kasai R, Lhieochaiphant S, Picheansoonthon C, Yamasaki K (1997) C-Glycosyl flavones from *Clinacanthus nutans* (Natural Medicine Note) 生藥學雜誌 51:557

Vigneshwaran N, Ashtaputre N, Varadarajan P, Nachane R, Paralikar K, Balasubramanya R (2007) Biological synthesis of silver nanoparticles using the fungus *Aspergillus flavus*. Mater Lett 61:1413–1418

Wayne P (2002) National committee for clinical laboratory standards. Perform Stand Antimicrob Disc Suscept Test 12:1–53